Supplementary Information

Crystal actuator based on a thermal phase transition and photothermal effect

Yuki Hagiwara,[a] Takuya Taniguchi,[b] Toru Asahi,[a,c] and Hideko Koshima*[c]

[a] *Department of Advanced Science and Engineering, Graduate School of Advanced Science and Engineering, Waseda University, 2-2 Wakamatsu-cho Shinjuku-ku, Tokyo 162-8480 (Japan)*
[b] *Center for Data Science, Waseda University, 27 Waseda-cho Shinjuku-ku, Tokyo 169-0042 (Japan)*
[c] *Research Organization for Nano & Life Innovation, Waseda University, 513, Waseda Tsurumakicho, Shinjuku-ku, Tokyo, 162-0041 (Japan)*

* Correspondence to h.koshima@kurenai.waseda.jp

Table of contents

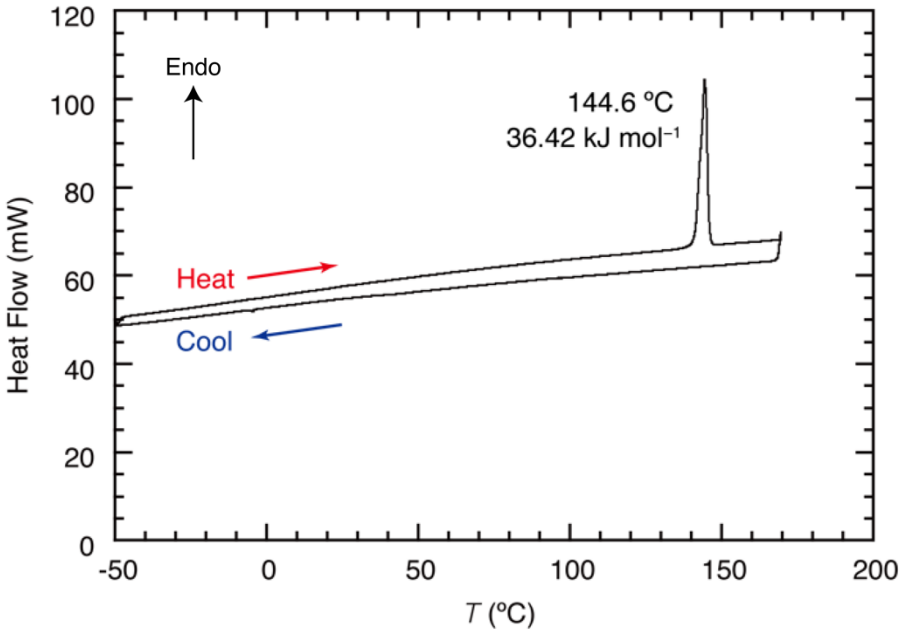

Fig. S1 Differential scanning calorimetry (DSC) curve of enol-**1** crystals measured in the temperature range from −50 to 170°C at a speed of 10°C min^{-1} upon heating and then cooling.

On heating, the endothermic peak corresponding to the melting point appeared at 144.6°C, but on subsequent cooling, any exothermic peak corresponding to the solidifying point of crystal did not appear due to the supercooling of the melt.

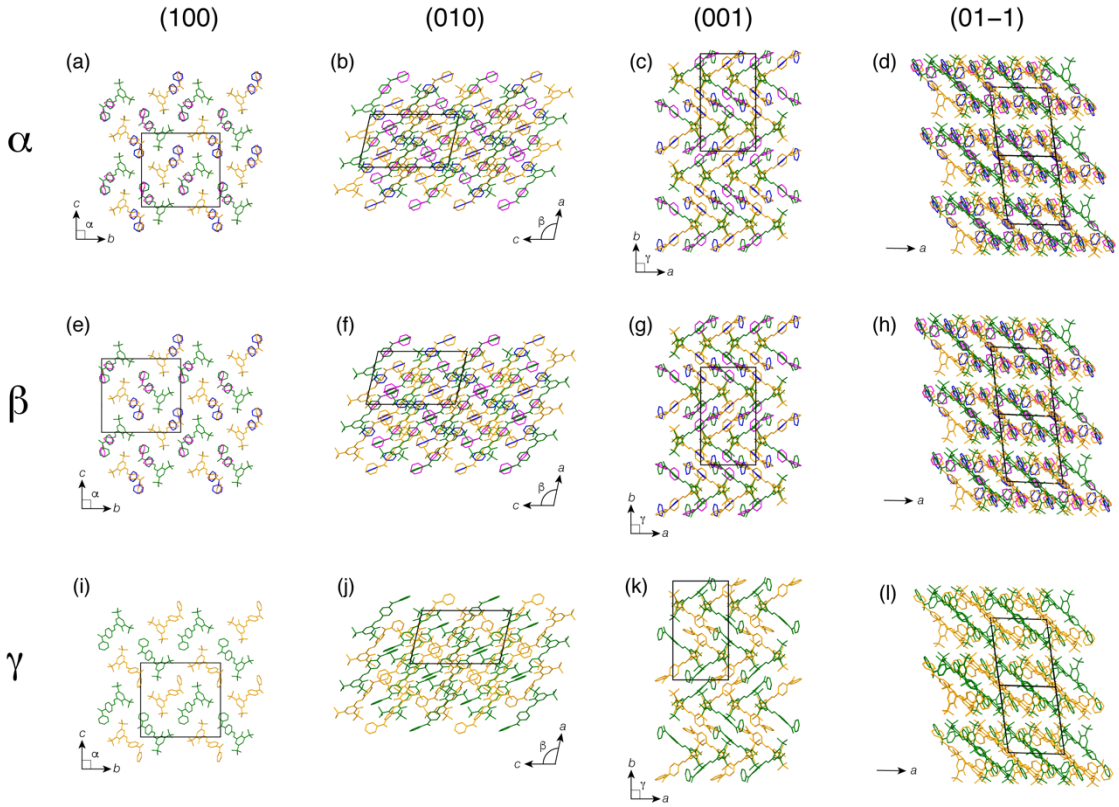

Fig. S2 Packing diagram in (a–d) α-, (e–h) β-, and (i–l) γ-phase, respectively; (a, e, i) (100), (b, f, j) (010), (c, g, k) (001), and (d, h, l) (01–1) faces. Hydrogen atoms are omitted for clarity.

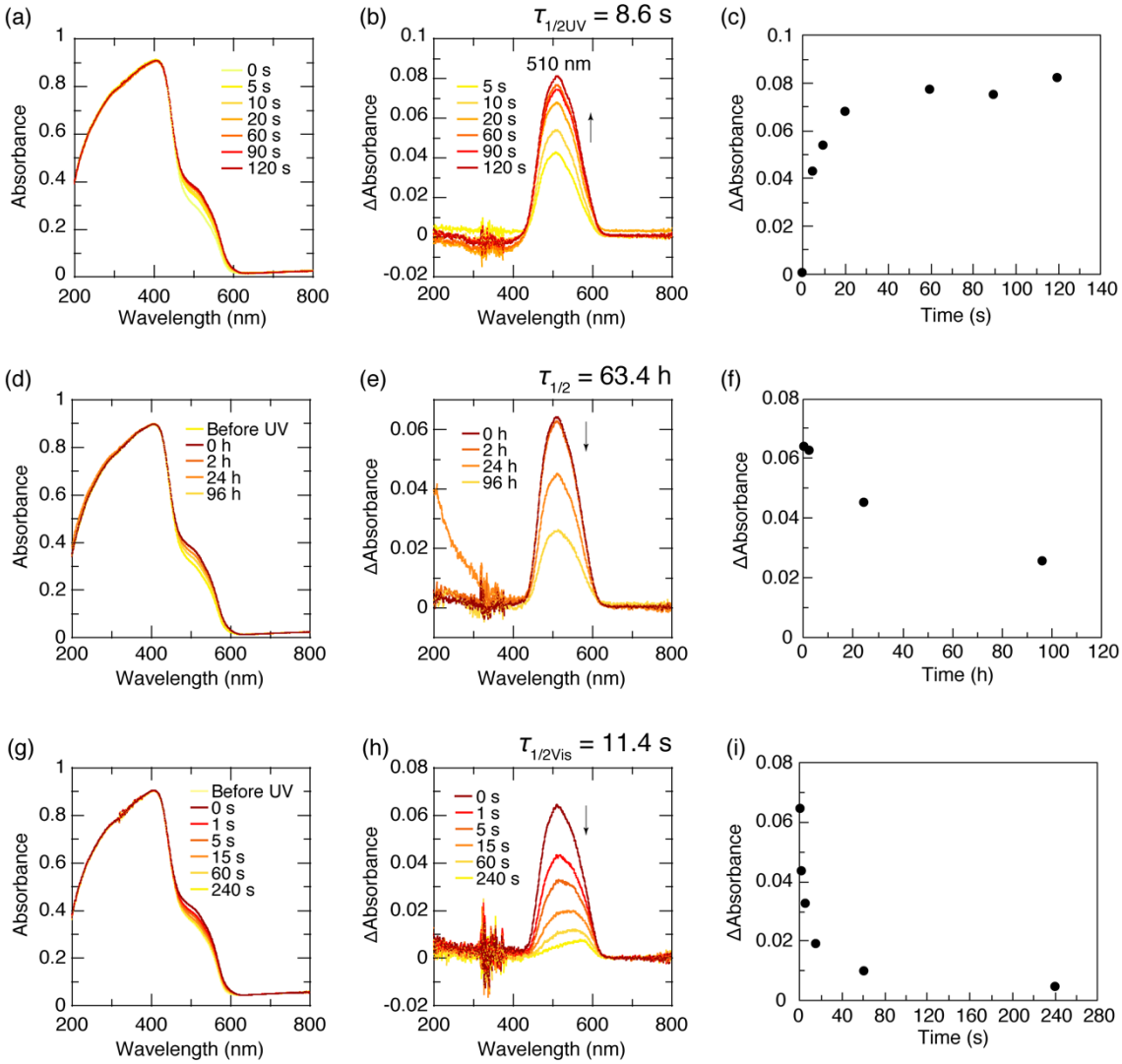

Fig. S3 (a, d, g) UV-Vis diffuse reflectance spectra and (b, e, h) difference spectra of enol-**1** in powdered crystals before and after UV light (365 nm, 40 mW cm^{-2}) irradiation at 20°C; (a, b) UV light irradiation, (c) time dependence of the absorbance at 510 nm, extracted from (b), (d, e) thermal relaxation after UV light irradiation for 2 min, (f) time dependence of the absorbance at 510 nm, extracted from (e), (g, h) visible light (488 nm, 5 mW cm^{-2}) irradiation after UV light irradiation for 2 min, (i) time dependence of the absorbance at 510 nm, extracted from (h). Difference spectra were obtained by subtracting the spectrum before UV light irradiation from the spectra after light irradiation.

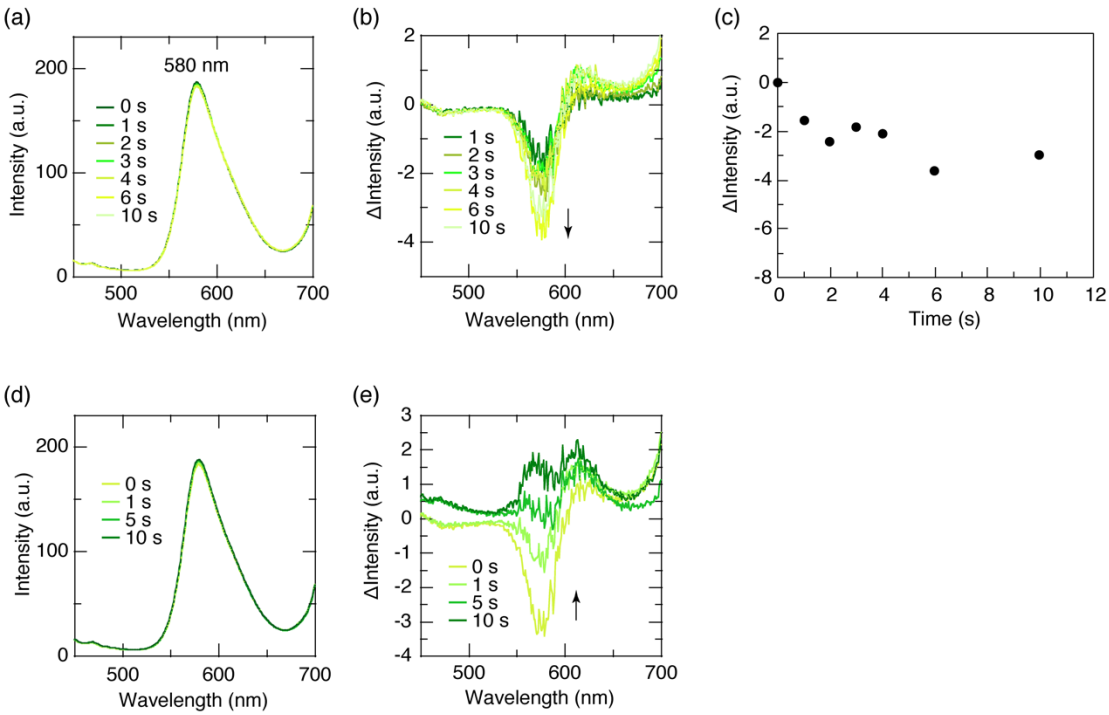

Fig. S4 (a, d) Fluorescence spectra (λ_{ex} = 365 nm) and (b, e) fluorescence difference spectra of enol-**1** in the crystals; (a, b) UV light (365 nm, 40 mW cm^{-2}) irradiation, (c) time dependence of the fluorescence intensity at 580 nm, extracted from (b), and (d, e) visible light (488 nm, 5 mW cm^{-2}) irradiation after UV light irradiation for 10 s. Difference spectra were obtained by subtracting the spectrum before UV light irradiation from the spectra after light irradiation.

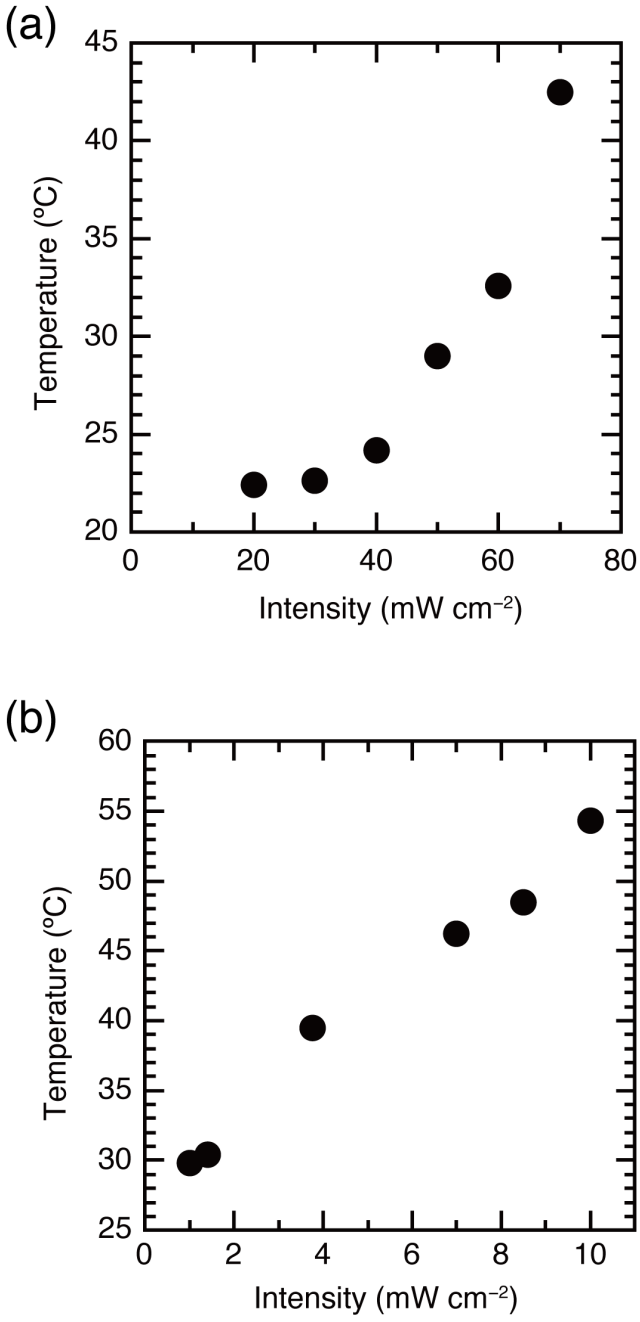

Fig. S5 Dependence of the light intensity on the surface temperature of the enol-**1** crystal upon (a) UV light (365 nm) irradiation at 20°C for 5 s, and (b) visible light (488 nm) irradiation at 30°C for 5 s.

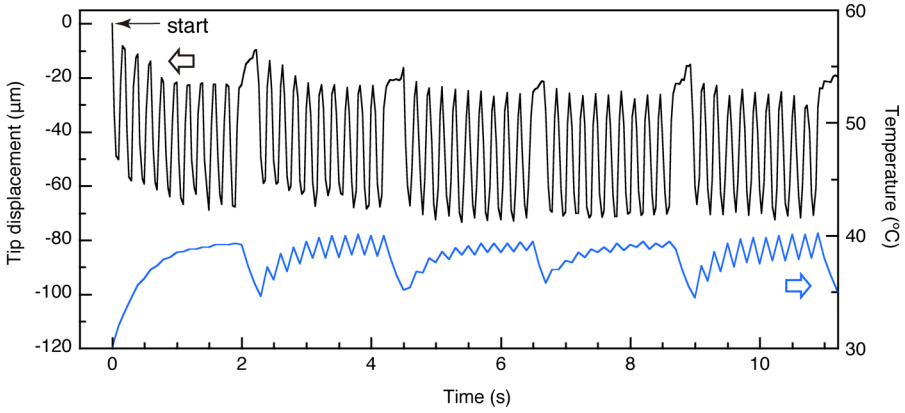

Fig. S6 Photothermal-based bending (5 Hz) of the γ-crystal at 30°C by repeating irradiation with the UV-LED light (365 nm, 70 mW cm^{-2}) for 0.1 s and stopping UV for 0.1 s.

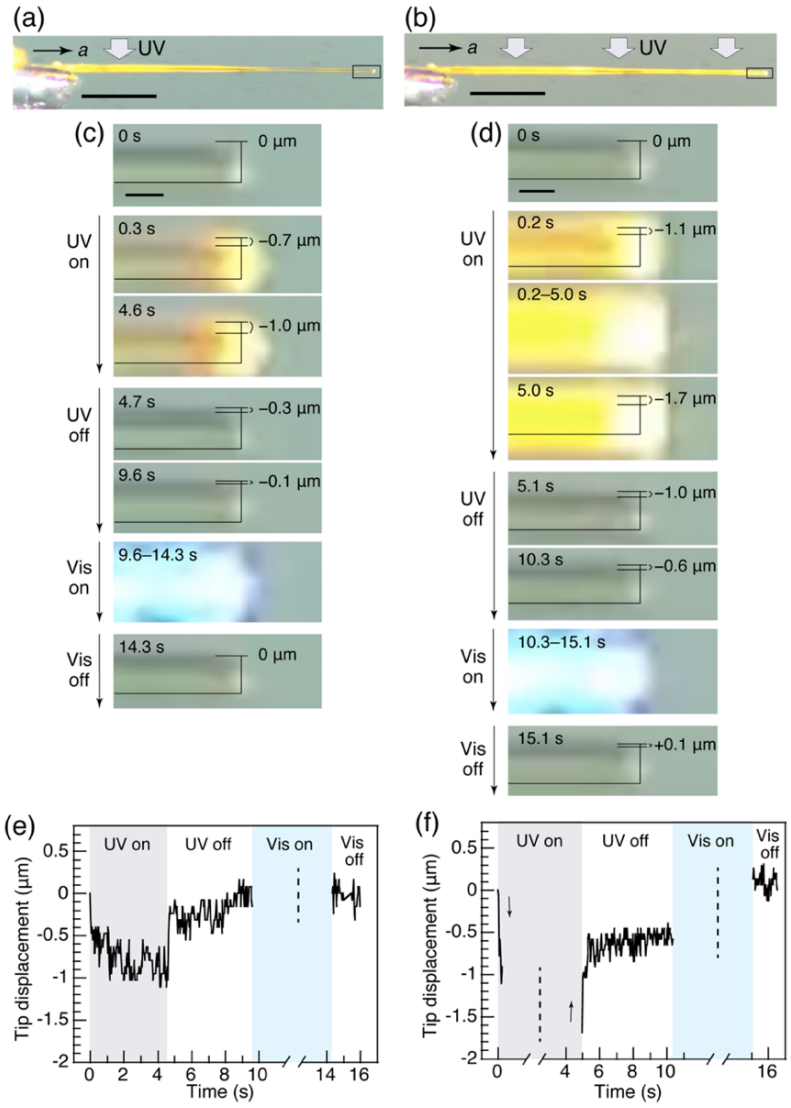

Fig. S7 Comparison of bending behaviour of the thin rod-like enol-**1** γ-microcrystal with the thickness of 5.4 µm upon UV laser (375 nm, 60 mW cm^{-2}) and visible light (488 nm, 8 mW cm^{-2}) irradiation to the left part of the crystal (a, c, e) and the entire crystal (b, d, f). (a, b) The microcrystal viewed from the side under UV laser irradiation. (c, d) Sequential snapshots of bending before, under, and after UV laser irradiation, and under and after visible light irradiation. (e, f) Time dependence of the right tip displacement. The scale bars in (a, b) and (c, d) are 100 and 5 µm, respectively.

The regions with the dotted lines in (e, f) indicate that the measurement of the tip displacement was difficult due to the yellow fluorescence emission from the microcrystal (Fig. 4) and the blue reflected light at the microcrystal surface during the irradiation to the entire microcrystal with UV and visible light, respectively.

(a)

	Before UV light (n = 10) Average ± Standard error	Under UV light (n = 10) Average ± Standard error
Formula	$C_{28}H_{31}O_2N$	$C_{28}H_{31}O_2N$
Size (mm^3)	0.5 × 0.2 × 0.2	0.5 × 0.2 × 0.2
Temp. (°C)	20	20
a (Å)	11.996 ± 0.001	11.998 ± 0.002
b (Å)	20.749 ± 0.003	20.760 ± 0.002
c (Å)	19.744 ± 0.002	19.742 ± 0.003
α (°)	89.97 ± 0.03	90.03 ± 0.02
β (°)	103.08 ± 0.03	103.07 ± 0.01
γ (°)	90.00 ± 0.02	89.95 ± 0.03
V ($Å^3$)	4786 ± 1	4790 ± 1

(b)

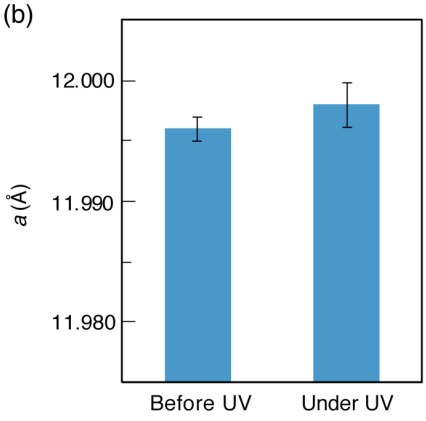

Fig. S8 (a) Changes of unit cell constants and (b) statistical evaluation of the change of *a*-axis length before and under UV light (365 nm, 60 mW cm^{-2}) irradiation at 20°C.

Repeated XRD measurements of the unit cell constants of the γ-crystal were performed 10 times before and under continuous irradiation with UV light. The results, as confirmed by statistical evaluation, revealed that the *a*-axis length (the longitudinal direction of the rod-like crystal) elongated slightly due to both the photoisomerization and photothermal effect under continuous UV irradiation.

Table S1. Crystal structures at various temperatures

Temperature (°C)	–100 (α)	–80 (α)	–60 (α)	–40 (α)	–20 (β)
Formula	$C_{28}H_{31}O_2N$	$C_{28}H_{31}O_2N$	$C_{28}H_{31}O_2N$	$C_{28}H_{31}O_2N$	$C_{28}H_{31}O_2N$
Formula weight	413.55	413.55	413.55	413.55	413.55
Crystal System	monoclinic	monoclinic	monoclinic	monoclinic	monoclinic
Space Group	$P2_1/n$	$P2_1/n$	$P2_1/n$	$P2_1/n$	$P2_1/n$
a (Å)	11.8902(10)	11.9470(13)	11.9648(11)	11.9783(13)	11.9400(9)
b (Å)	20.4055(17)	20.4908(22)	20.5178(10)	20.5630(2)	20.6089(16)
c (Å)	19.5881(19)	19.6729(24)	19.6900(20)	19.7170(3)	19.6385(16)
α (°)	90	90	90	90	90
β (°)	102.618(7)	102.528(7)	102.445(7)	102.423(7)	102.854(7)
γ (°)	90	90	90	90	90
Z	8	8	8	8	8
Z'	2	2	2	2	2
V (Å^3)	4637.8(7)	4701.3(9)	4720.1(8)	4742.9(10)	4711.3(6)
d_{calc} (g/cm^3)	1.185	1.185	1.164	1.158	1.166
R_1 (I>2σ(I))	0.0698	0.0897	0.0965	0.1055	0.0727
wR_2	0.2146	0.2058	0.3094	0.2622	0.2230
GOF	0.979	1.011	1.004	1.018	1.027

Temperature (°C)	0 (β)	10 (β)	20 (γ)	40 (γ)	60 (γ)
Formula	$C_{28}H_{31}O_2N$	$C_{28}H_{31}O_2N$	$C_{28}H_{31}O_2N$	$C_{28}H_{31}O_2N$	$C_{28}H_{31}O_2N$
Formula weight	413.55	413.55	413.55	413.55	413.55
Crystal System	monoclinic	monoclinic	monoclinic	monoclinic	monoclinic
Space Group	$P2_1/n$	$P2_1/n$	$P2_1/n$	$P2_1/n$	$P2_1/n$
a (Å)	11.9560(7)	11.9551(14)	11.9580(6)	11.9775(6)	11.9960(6)
b (Å)	20.6140(14)	20.612(3)	20.6959(12)	20.7298(12)	20.7564(13)
c (Å)	19.6672(10)	19.666(2)	19.6827(13)	19.7194(9)	19.7939(11)
α (°)	90	90	90	90	90
β (°)	102.850(7)	102.907(7)	103.024(7)	102.934(7)	102.759(7)
γ (°)	90	90	90	90	90
Z	8	8	8	8	8
Z'	2	2	2	2	2
V (Å^3)	4725.8(5)	4723.6(10)	4745.8(5)	4771.9(4)	4792.3(5)
d_{calc} (g/cm^3)	1.162	1.163	1.158	1.151	1.146
R_1 (I>2σ(I))	0.0884	0.0666	0.0721	0.0965	0.1069
wR_2	0.2478	0.2206	0.2047	0.2525	0.2665
GOF	1.023	0.832	0.912	1.036	1.065

Movie S1: Bending of a long rod-like enol-**1** crystal with a thickness gradient on heating and then cooling in the temperature range from 16 to 43°C at a rate of 0.4°C s^{-1} observed by a microscope (played at 10× speed).

Movie S2: Bending of a long rod-like enol-**1** crystal with uniform thickness, of which left part was placed on a glass, on heating and then cooling in the temperature range from 17 to 40°C at a rate of 0.3 and 0.4°C s^{-1}, respectively, observed by a microscope and simultaneous monitor of surface temperature distribution by an IR thermography camera (played at 10× speed).

Movie S3: Bending of a long rod-like crystal with uniform thickness, of which left part was placed on a glass at 15°C, upon UV-LED light (365 nm, 70 mW cm^{-2}) irradiation to the left part, observed by a microscope and simultaneous monitor of surface temperature distribution by an IR thermography camera (Realtime).

Movie S4: Bending of a long rod-like crystal with uniform thickness, of which left part was placed on a glass at 15°C, upon visible light (488 nm, 10 mW cm^{-2}) irradiation to the left part (Realtime).

Movie S5: High frequency bending actuation (25 Hz) of a long rod-like crystal with uniform thickness, of which left part was placed on a glass at 30°C, by pulsed-like irradiation of the UV laser light (375 nm, 70 mW cm^{-2}) to the left part, observed by a microscope (played at 0.25× speed).